



**Ratiometric mechanosensitive fluorescent dyes: Design and applications**

Journal:	<i>Journal of Materials Chemistry C</i>
Manuscript ID	TC-REV-10-2015-003504.R1
Article Type:	Review Article
Date Submitted by the Author:	16-Dec-2015
Complete List of Authors:	Haidekker, Mark; University of Georgia, College of Engineering Theodorakis, Emmanuel; University of California, San Diego, Department of Chemistry and Biochemistry



## Journal of Materials Chemistry C

## REVIEW

Received 00th January 20xx,  
Accepted 00th January 20xx

DOI: 10.1039/x0xx00000x

[www.rsc.org/](http://www.rsc.org/)



Mark Andreas Haidekker is a Professor at the College of Engineering at the University of Georgia. He completed his five-year university degree (Diploma) in Electrical Engineering at the University of Hannover, Germany. After five years in industry, he returned to graduate school and received his doctoral degree in Computer Science from the University of Bremen, Germany. From 1999 to 2001, he was employed at the University of California, San Diego first as postdoctoral fellow, then as research scientist. In 2002 he became an Assistant Professor at the Department of Biological Engineering at the University of Columbia, Missouri. In 2007, he assumed his present position. His interests are biomedical imaging, sensing and instrumentation.



Emmanuel A. Theodorakis received his B.S. Degree in Chemistry from the University of Athens and his M.S. Degree (D.E.A.) and Ph.D. Degree in Organic Chemistry from Paris XI University (France). His M.Sc. studies were performed at the Institute of Chemistry of Natural Products (ICSN-CNRS) under the direction of Professor H.-P. Husson, while his Ph.D. studies were performed at Texas A&M University under the direction of Sir Derek H. R. Barton. Following a postdoctoral appointment at TSRI in the laboratories of Professor K. C. Nicolaou, in 1995 he joined the faculty at UCSD where he is currently a Professor and the T.G. Traylor Scholar at the Department of Chemistry and Biochemistry. His research focuses on the synthesis and biological studies of natural products and development of small molecules as probes in imaging and sensing.

<sup>a</sup> College of Engineering, University of Georgia, 597 D. W. Brooks Drive, Athens, GA 30602, USA. Email: [mhaidekk@uga.edu](mailto:mhaidekk@uga.edu)

<sup>b</sup> Department of Chemistry & Biochemistry, University of California, San Diego, 9500 Gilman Drive MC: 0358, La Jolla, CA 92093-0358, USA. Fax: 1-858-822-0386; Tel: 1-858-822-0456; Email: [etheodor@ucsd.edu](mailto:etheodor@ucsd.edu)

# Ratiometric mechanosensitive fluorescent dyes: Design and applications

Mark A. Haidekker<sup>a\*</sup> and Emmanuel A. Theodorakis<sup>b\*</sup>

Fluorescent molecules, with their almost instantaneous response to external influences and relatively low-cost measurement instrumentation, have been attractive analytical tools and biosensors for centuries. More recently, advanced chemical synthesis and targeted design have accelerated the development of fluorescent probes. This article focuses on dyes with segmental mobility (known as fluorescent molecular rotors) that act as mechanosensors, which are known for their relationship of emission quantum yield with microviscosity. Fluorescence lifetime is directly related to quantum yield, but steady-state emission intensity is not. To remove confounding factors with steady-state instrumentation, dual-band emission dyes can be used, and molecular rotors have been developed that either have intrinsic dual emission or that have a non-sensitive reference unit to provide a calibration emission band. We report on theory, chemical structure, applications and targeted design of several classes of dual-emission molecular rotors.

## 1. Introduction

The phenomenon of fluorescence has almost 500 years of history with the first observations described in 1560 by Bernardino de Sahagun and Monardes who were studying an infusion known as *lignum nephriticum*.<sup>1</sup> The term *fluorescence* was proposed by Stokes in 1852 to describe the dispersion of light when passing through a solution of quinine.<sup>2</sup> In subsequent studies, Pierre showed that the fluorescent spectrum of a compound can be changed as a function of the solvent and reagents,<sup>3</sup> while Goppelsröder first proposed the concept of *fluorescence analysis*.<sup>4</sup> Since these ground-breaking contributions, the field of fluorescence has expanded dramatically with concurrent advances in chemistry, biology and engineering to address issues related to the study of living systems and personalized medicine. In fact, two recent Nobel Prize awards, for the discovery and development of the Green Fluorescent Protein (2008)<sup>5</sup> and for the development of super-resolved fluorescent microscopy (2014)<sup>6</sup> epitomize such advances. In turn, the quest for new fluorophores with increased versatility, sensitivity and quantitative capabilities continues to expand.<sup>7</sup>

As compared to other methods, such as isotope labeling, magnetic resonance imaging, electron spin resonance and electrochemical detection, fluorescence imaging is advantageous due to its high sensitivity, minimal invasiveness and safe detection.<sup>8</sup> Small molecule-based fluorescent probes have become indispensable tools in biology since they can provide dynamic information, such as localization and quantification of the molecules of interest without the need for genetic engineering of the sample.<sup>9, 10</sup> In general, issues related to localization can be addressed by combining a binding unit that selectively recognizes a target analyte with a fluorescent chromophore that is sensitive to the presence of the target. Translating a given fluorescence response to quantity of analyte requires the response to be independent of external factors (e.g. light source, light path geometry, sample bleaching, concentration etc) but also chromophore concentration.<sup>11</sup>

The above challenges have prompted the development of dyes with dual emission that either present an isosbestic point

or an environment-independent emission band for calibration. In this article, we focus on environment-sensitive dyes (specifically, a class of dyes with segmental mobility referred to as *fluorescent molecular rotors*), which have gained tremendous popularity as microscale viscosity sensors.<sup>12</sup> Molecular rotors with dual emission and compound dyes with reference emission have recently gained some attention. In this article, we provide the foundation for measurements with dual-emission dyes, and we present criteria that guide the rational design of such ratiometric dye systems. We also show some applications, discuss how these applications impose additional design constraints, and we compare engineered dual-emission dyes to alternative concepts realized with related dyes.

## 2. Dual-emission fluorophores

The significance of dual-emission dyes stems from their ability to cancel out several external factors that influence emission intensity. For low dye concentrations, an approximate relationship between emission intensity  $I_{em}$  and quantum yield  $\Phi_F$  can be given as

$$I_{em} = I_{ex} \cdot c \cdot g \cdot \Phi_F \quad (1)$$

where  $I_{ex}$  is the intensity of the excitation beam,  $c$  the dye concentration, and  $g$  an instrument-specific factor that combines the instrument's geometry and collection efficiency, and the instrument's sensor and gain factors.<sup>13</sup> Many spectroscopic instruments provide intensities as unitless values, primarily on account of  $g$ . Even photon-counting instruments are subject to instrument-specific geometry and collection efficiency, and the value of  $g$  is usually unknown. Although calibration with quantum yield standards is sometimes possible for spectrometers, the task becomes extremely challenging for fluorescent microscopes where the illumination field is non-homogeneous and local concentrations can vary within the sample. If a second and distinctly separate emission peak exists – we can think of it as a reference emission  $I_{ref}$  – the ratio of the two emissions

becomes independent of local concentration and instrument factors:

$$\frac{I_{em}}{I_{ref}} = \frac{I_{ex} \cdot c \cdot g \cdot \Phi_F}{I_{ex} \cdot c \cdot g \cdot \Phi_{ref}} = \frac{\Phi_F}{\Phi_{ref}} \quad (2)$$

This concept remains valid when the second emission is not a constant reference but rather varies with environmental factors. Two examples are the well-known dual-emission dyes 6-propionyl-2-dimethylaminonaphthalene (PRODAN, **1**)<sup>14</sup> and 1-anilinonaphthalene-6-sulfonic acid (ANS, **3**)<sup>15</sup> (Fig. 1). Both dyes are polarity probes due to the formation of excited-state intramolecular charge transfer (ICT) complexes, and both dyes continuously shift their emission wavelength from approximately 400 nm in apolar solvents to 460 nm (ANS) and 525 nm (PRODAN) in highly polar media, such as water (Fig. 2A).<sup>16</sup> To illustrate the concept given in Equation 2, the hydrophobic PRODAN derivative LAURDAN (6-dodecanoyl-2-dimethylaminonaphthalene, **2**) is a well-known cell membrane dye, and the polarity of the cell membrane is quantified by general polarization (GP), which is defined as the difference of the emission intensities at 435 nm and 500 nm divided by the sum of these intensities.<sup>17</sup> Since the factors  $I_{ex}$ ,  $c$  and  $g$  are common to both intensities, they cancel out in the value of GP (Fig. 2).

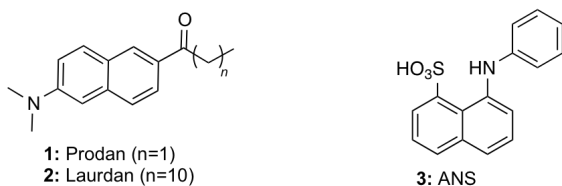


Fig. 1. Chemical structures of PRODAN, LAURDAN and ANS

Selected additional examples of dual-emission fluorophores are highlighted in Fig. 3. For instance, *N*-phenyl-2,3-naphthalimide (**4a**) was found to exhibit dual emission at approximately 400 and 500 nm that originate from a molecular conformation in which the phenyl and naphthalimide rings are either orthogonal or coplanar to each other.<sup>18</sup> Nandhikonda and Heagy have shown that incorporating various substituents at the periphery of the naphthalimide core can produce fluorescent dyes with interesting applications.<sup>19</sup> For example, compound **4b** exhibits a dual emission that is conducive to ratiometric detection of DNA and suitable for applications in white-light emitting fluorophores.<sup>19a</sup> On the other hand, compound **4c** was designed to bind to the  $\alpha$ -helical region of cardiac troponin I allowing its ratiometric detection at clinically relevant concentrations.<sup>19c</sup> Similarly, peripheral functionalization of the related *N*-aryl-1,8-naphthalimide scaffold (**5a**) produces fluorescent dyes for various applications.<sup>20</sup> As compared to **5a**, the pyridyl derivative **5b** was shown to shift both absorption and emission bands toward the red, while attachment of a boronic acid unit at the phenyl ring produced compound **5c** that is amenable to ratiometric detection of carbohydrates.<sup>21</sup>

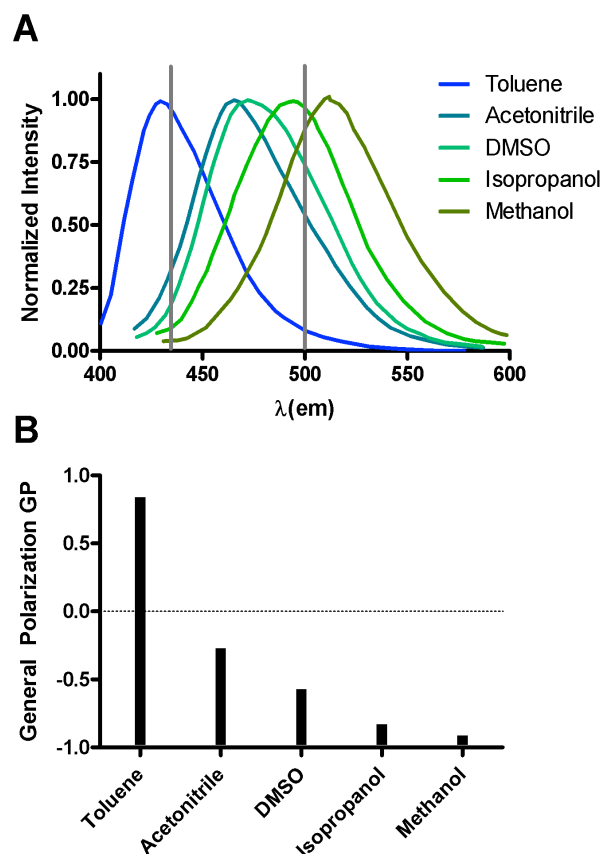


Fig. 2 (A): Emission spectra of PRODAN in different solvents. The gray lines indicate the wavelength points from which the general polarization is computed. (B) General Polarization (GP) values for the different solvents. GP values vary from +1 to -1 with increasing polarity.

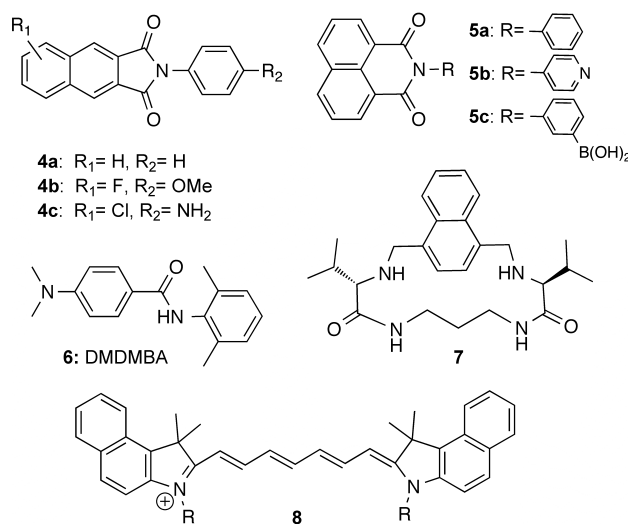


Fig. 3. Chemical structures of selected dual-emission fluorophores

Dual fluorescence was observed in various organic solvents with aminobenzanilide derivatives such as DMDMBA (**6**). In this case, the charge-transfer (CT) emission shifted to the red with increasing solvent polarity from cyclohexane (480 nm) to diethyl ether (520 nm).<sup>22</sup> A blue shift was observed between

diethyl ether and THF (424 nm) and a bathochromic shift in acetonitrile (484 nm). This unusual behavior was ascribed to two competitive CT channels, one whose CT reaction occurs from the amido aniline to benzoyl moiety in nonpolar solvents and the other from the dimethylamino group to the benzanilide in polar solvents. Similarly, dual fluorescence emission has been recorded for certain azulene derivatives.<sup>23</sup>

Dual-emission dyes, such as the examples above, have found significant applications as chemosensors for metals, such as calcium,<sup>24</sup> lead,<sup>25</sup> zinc,<sup>26</sup> copper<sup>27</sup> but also for biomolecular building blocks,<sup>28</sup> such as amino acids,<sup>29</sup> nucleic acids<sup>30</sup> and carbohydrates.<sup>31</sup> One representative example of a fluorescent chemosensor is presented in Fig. 3. Cyclophane derivative **7** has been reported to bind to carboxylic acids in organic media and change its emission in a ratiometric fashion.<sup>32</sup> This compound displays dual emission at 330 and 390 nm when excited at 300 nm in dichloromethane. On the other hand, compound **8** is a representative of a near-infrared dye that fluoresces at two different wavelengths, approximately at 700 and 800 nm, (dichromic fluorescence). Dye **8** was shown to bind to protein kinase B and quantitatively report this enzyme's activity in real time.<sup>33</sup> Induction of structural asymmetry amplifies the dichromic fluorescence and provides an interesting contrast mechanism to detect and quantify activities of biomolecules in cells and tissues.

### 3. Fluorescent molecular rotors

Fluorescent molecular rotors are an emerging class of environment-sensitive fluorophores that are defined by their ability to undergo an intramolecular twisting motion in their excited state.<sup>34</sup> The first recognized and widely studied fluorescent molecular rotor is 4,4-dimethylaminobenzonitrile (DMABN, **9**) (Fig. 4). The intriguing fluorescence behaviour of **9** was initially attributed by Lippert *et al* to solvent-induced reversal of polarization states.<sup>35</sup> More recently, Rotkiewicz and Grabowsky proposed that the fluorescence of **9** is due to the existence of twisted intramolecular charge transfer (TICT) states.<sup>34, 36</sup> This hypothesis provides a general model for all fluorescent molecular rotors. In parallel, Förster and Hoffmann proposed a theory, based on the classical Debye-Stokes-Einstein microfriction concept, which quantitatively explained the relationship between solvent microviscosity and emission quantum yield of dyes with their ability to perform intramolecular rotation.<sup>37</sup> These fluorescent dyes have rapidly gained high popularity as viscosity sensors in many fields, such as, for example, in cells and model membranes<sup>38</sup>, to monitor polymerization processes<sup>39</sup> and to observe protein conformation and assembly.<sup>40</sup>

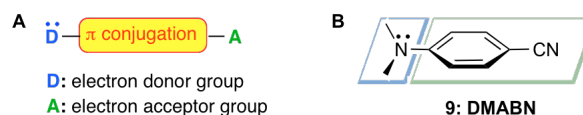


**Fig. 4 (A): General structure of a fluorescent molecular rotor.** The electron donor group is represented by D, and the acceptor group by A. Intramolecular charge transfer takes place from the donor to the acceptor motif and an intramolecular rotation of the acceptor with respect to the donor is possible. **(B): Chemical structure of DMABN (9) showing the two different planes of the donor and acceptor groups.** The lowest-energy ground-state conformation, where the benzene and dimethylamino planes are approximately parallel, can be converted into a higher-energy twisted conformation, where the two planes are perpendicular to each other, by rotation around the nitrogen-benzene single bond.

Typically, the structure of a fluorescent molecular rotor is composed of an electron donor group that is in conjugation with an electron acceptor group through a network of alternating single and double bonds (Fig. 4A). At the ground state ( $S_0$ ), the  $\pi$ -orbitals are aligned due to an extended conjugation and thus, the molecule adopts a planar (or near planar) conformation, which is the lowest energetic conformation (Fig. 4B). Upon photoexcitation at wavelength  $\lambda_{\text{ex}}$  the dye undergoes intramolecular charge transfer from the donor to acceptor, whereby it reaches a planar locally-excited state ( $S_1^{\text{LE}}$ ). Under the influence of the excited state charge separation, the molecule rapidly twists around a single bond and assumes the lowest energy conformation of the excited state ( $S_1^{\text{TICT}}$ ) (Fig. 5). This intramolecular rotation occurs around the  $\sigma$ -bonds that connect the electronically rich donor with the acceptor.

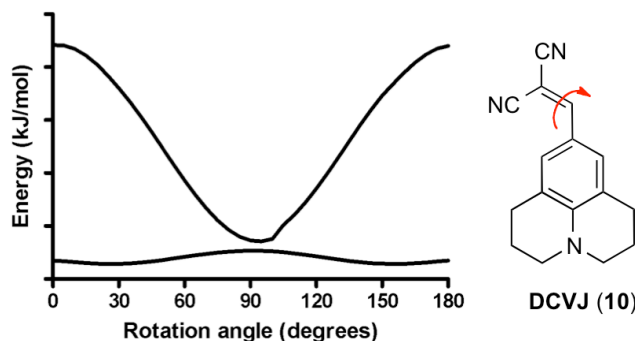


**Fig. 5. Energy surface typical for a fluorescent molecular rotor, such as DCVJ (10), in the ground and excited state as a function of the rotation angle around a single bond.<sup>41</sup>**

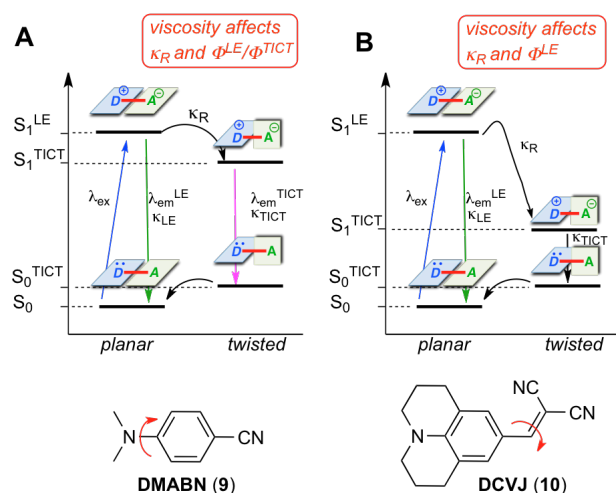


**Fig. 6.** Extended Jablonski diagram showing TICT states and kinetics for fluorescent molecular rotors. (A) Dual emission case (e.g., DMABN, **9**): Photoexcitation with  $\lambda_{\text{ex}}$  (blue arrow) leads to a locally-excited planar state ( $S_1^{\text{LE}}$ ) from where fluorescent relaxation occurs with deexcitation rate  $\kappa_{\text{LE}}$  and  $\lambda_{\text{em}}^{\text{LE}}$  (green arrow). Depending on the solvent viscosity, the dye can undergo intramolecular twisting with rate  $\kappa_{\text{R}}$  to enter a twisted excited state ( $S_0^{\text{TICT}}$ ) from where it can relax by photon emission with a deexcitation rate  $\kappa_{\text{TICT}}$  and a red-shifted  $\lambda_{\text{em}}^{\text{TICT}}$  (red arrow). (B) Single emission case (e.g., DCVJ, **10**): In this case, the energy difference between  $S_1^{\text{TICT}}$  and  $S_0^{\text{TICT}}$  is too small for photon emission, thus the dye deexcites from the twisted state via non-radiative processes (black arrow) and emits only a single emission band at wavelength  $\lambda_{\text{em}}^{\text{LE}}$  whose quantum yield increases with increasing solvent viscosity.

Usually, the intramolecular rotation rate ( $\kappa_{\text{R}}$ ) is higher than the fluorescence deexcitation rate ( $\kappa_{\text{LE}}$ ) and thus, the quantum yield from the  $S_1^{\text{LE}}$  state is very low (Fig 6). From the twisted conformation, deexcitation occurs with photon emission at  $\lambda_{\text{em}}^{\text{TICT}}$ . Since the energy difference between excited and ground state is lower in the twisted than in the planar conformation, photon emission from the twisted conformation is red-shifted over emission from the LE conformation ( $\lambda_{\text{em}}^{\text{TICT}} > \lambda_{\text{em}}^{\text{LE}}$ ). Along these lines, hindrance of intramolecular rotation can be interpreted as an increase of the energy barrier between planar and twisted excited-state which reduces the  $\kappa_{\text{R}}$  and thus favors deexcitation from the planar conformation. In fact, in the extreme case of glass-forming solvents at 77 °K, the dye cannot rotate and thus it emits exclusively from the  $S_1^{\text{LE}}$  state with a quantum yield of near unity.<sup>42</sup>

As shown in Fig. 6A, two channels account for the relaxation of the excited fluorescent molecular rotor to the planar ground state. The first channel involves direct deexcitation with photon emission from the  $S_1^{\text{LE}}$  to the  $S_0$  state and reflects the fluorescent behavior of conventional intramolecular charge-transfer (ICT) fluorophores. The second channel involves intramolecular twisting to the  $S_1^{\text{TICT}}$  followed by relaxation to the  $S_0^{\text{TICT}}$  state via photon emission and subsequent non-radiative relaxation to the planar  $S_0$  state. Photon emission from the second channel takes place when the  $S_1^{\text{TICT}} - S_0^{\text{TICT}}$  energy gap is large enough (roughly 1.5-3.0 eV for photons in the visible to near-infrared range) and produces a distinct red-shifted second emission band ( $\lambda_{\text{em}}^{\text{TICT}} > \lambda_{\text{em}}^{\text{LE}}$ ). DMABN, for example, has a distinct dual emission due to

radiative relaxation from both the  $S_1^{\text{LE}}$  and the  $S_1^{\text{TICT}}$  states. Conversely, if the  $S_1^{\text{TICT}} - S_0^{\text{TICT}}$  energy gap is very small, no photons are emitted from the  $S_1^{\text{TICT}}$  state to the  $S_0^{\text{TICT}}$  and ultimately to the planar ground state (Fig 6B). Fluorophores with this profile, such as DCVJ (**10**), exhibit a single emission band at wavelength  $\lambda_{\text{em}}^{\text{LE}}$ .

The environmental sensitivity of fluorescent molecular rotors can be rationalized by considering: (a) the effect of solvent polarity to the stability of the polar excited state; and (b) the effect of solvent microviscosity to the ability of the excited dye to undergo intramolecular twisting, i.e. the intramolecular rotation rate  $\kappa_{\text{R}}$ . Polar solvents stabilize the  $S_1^{\text{TICT}}$  state over the  $S_1^{\text{LE}}$  state. In addition, due to the larger dipole moment of the excited TICT state, they cause a stronger bathochromic shift of the TICT emission as compared to the LE emission. On the other hand, viscous solvents increase the energy barrier between planar and twisted states, which reduces intramolecular rotation rate ( $\kappa_{\text{R}}$ ) and thus favors deexcitation from the  $S_1^{\text{LE}}$  state.

In dyes like DCVJ (**10**) that exhibit non-radiative emission from the twisted excited state, the fluorescence quantum yield (from the planar excited state) increases by increasing the viscosity of the solvent. In this latter case, the quantum yield  $\Phi_{\text{F}}$  is known to obey a power-law relationship with the solvent viscosity

$$\Phi_{\text{F}} = \Phi_0 \left( \frac{\eta}{\sigma} \right)^x \quad (3)$$

where  $\Phi_0$  is the dye's intrinsic quantum yield,  $\sigma$  is a dye constant, and  $x$  depends on both dye and solvent. This relationship, often referred to as the Förster-Hoffmann equation,<sup>37</sup> holds over several magnitudes of viscosity. Equation (3) could be used to calculate the solvent's viscosity from a measured quantum yield. Fluorescent quantum yield  $\Phi_{\text{F}}$  and lifetime  $\tau$  are directly related through

$$\Phi_{\text{F}} = \frac{\tau}{\tau_{\text{N}}} \quad (4)$$

where  $\tau_{\text{N}}$  is the natural lifetime, that is, the lifetime in the absence of nonradiative deexcitation. Measurement of a fluorophore's lifetime allows to calculate its quantum yield and, in turn, the microviscosity of the environment.<sup>43</sup> Many fluorescent molecular rotors show a low quantum yield in most solvents and their fluorescence lifetime can be in the range of 100 ps or less. Lifetime instrumentation can be rather complex for fluorophores whose lifetime is far below the nanosecond range, thus steady-state instrumentation is more commonly used. Since steady-state instruments generally measure emission intensity, quantum yield is not easily accessible because emission intensity depends not only on  $\Phi_{\text{F}}$ , but also on a number of external factors, such as fluorophore concentration, excitation intensity, absorption along the optical path, and instrument collection efficiency and gain (Equation 1). Steady-state fluoroscopy is therefore limited to relative measurements. Such limitations can be overcome if a second emission exists that can serve as calibration or reference emission. Ideally, the second emission band would

exhibit different environment-sensitive behaviour than the first so that some optical factors (see Section 6 for more details) can be removed from the measurement.

#### 4. TICT fluorophores with dual emission

Some molecular rotors exhibit natural emission in two bands. As briefly presented in section 2, DMABN (**9**) exhibits dual emission due to: (a) the larger  $S_1$ - $S_0$  energy gap in the planar conformation leading to emission at 350 nm; and (b) the reduced  $S_1$ - $S_0$  energy gap in the twisted conformation causing an emission at 450 nm. The red-shifted band is more susceptible to solvent polarity, while solvents of higher viscosity decrease the quantum yield of the red-shifted band and increase that of the blue-shifted band.

Selected examples of TICT fluorophores with dual emission are illustrated in Fig. 7. Methylation of adenosine at the N<sup>6</sup> position produces DMA (**11**) that exhibits dual fluorescence emission at 330 and 500 nm.<sup>44</sup> The red-shifted emission is proposed to derive from the TICT state and dominates in aprotic solvents but is quenched in protic solvents. The fluorescence quantum yield of the short wavelength emission increases by three orders of magnitude when the temperature is lowered at 80 °K in accordance with the behaviour of normal nucleic acid bases, while the fluorescence emission from the TICT state is temperature independent. Likewise, the dual fluorescence of N-ethyl isoquinolinium **12** results from two nearby excited states in which the ethyl group of the nitrogen can reside parallel or perpendicular to the aromatic ring.<sup>45</sup>

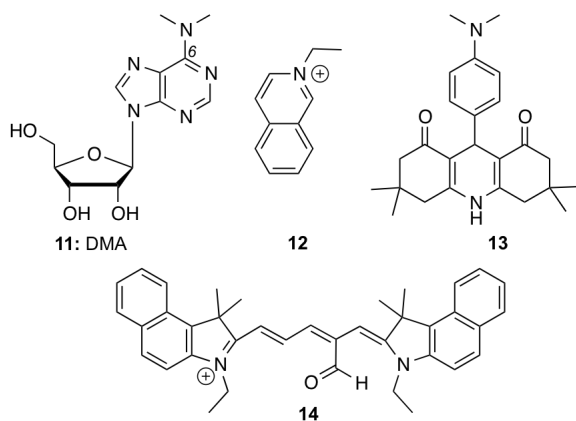


Fig. 7. Chemical structures of representative single TICT fluorophores with dual emission

For similar reasons, *N,N*-dimethylated aniline-acridinedione conjugate **13** (Fig. 7) exhibits dual emission in aprotic solvents and a single emission in protic solvents.<sup>46</sup> The presence of two different conformations of this molecule at the ground state leads to two close-lying excited states thereby resulting in dual fluorescence. A charge transfer state has been identified as the source of the long wavelength anomalous fluorescence.

Compound **14** (Fig. 7) represents an interesting example of a pentamethine dye containing a rotating aldehyde group.<sup>47</sup>

This compound exhibits dual emission at 456 and 650 nm likely due to intramolecular charge transfer to an energetically higher orbital (LUMO+1 or  $S_2$  excited state) from which deexcitation leads to emission at 456 nm. A rotation of the aldehyde group by 90° reduces the energy level to the  $S_1$  excited state from which radiative emission occurs at 650 nm. Interestingly, this pentamethine dye has also two absorption bands at 400 nm (related to the  $S_0$ - $S_2$  transition) and 600 nm, related to the  $S_0$ - $S_1$  transition. The ratio of the emission intensities at 650 and 456 nm shows power-law relationship to solvent viscosity. Due to its hydrophilic character, this dye was proposed for cell viscosity imaging.

Compound **15** represents an application of a TICT fluorophore with dual emission for the ratiometric sensing of amino acids (Fig. 8).<sup>48</sup> Placement of an amino acid sensor, composed of a guanidinium ion and a crown ether, in proximity to a TICT dye, based on the dimethylamino benzoic acid structure, via a rigid scaffold such as cholic acid,<sup>49</sup> produces sensor **15**. The design is based on the principle that binding of an amino acid to the sensor unit would induce changes in the polarity and/or steric hindrance around the TICT fluorophore thus altering the ratio of TICT/LE fluorescence emission. Indeed, this intensity ratio decreased with an increase in the concentration of *N*-acetyl-D-phenylalanine. Based on these experiments the apparent binding constant of this amino acid was determined at 7.0  $\mu$ M.

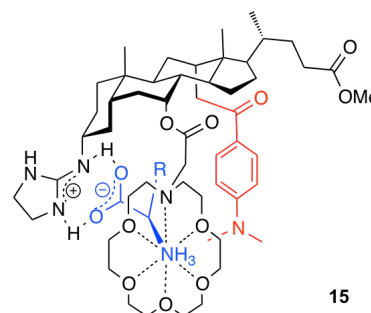


Fig. 8. Representative structure of an amino acid sensor based on the TICT dual emission concept. The TICT motif is shown in red while the amino acid analyte is shown in blue. The sensor tends to fold in the presence of an amino acid, thereby restricting the intramolecular rotation of the TICT motif.

Porphyrin-based fluorescent molecular rotors with dual emission have recently been reported. Kuimova *et al.* reported a porphyrin dimer **16** (Fig. 9) that can rotate around the linear diyne linker and shows two emission bands, at 710 nm and 780 nm.<sup>50</sup> Similarly to single-emission fluorescent molecular rotors, the ratio of their intensities shows a power-law relationship with solvent viscosity. The remarkable non-linear optical properties, high intracellular uptake, photostability and favorable photophysical properties of **16** open the way for potential applications in photodynamic therapy of cancer.<sup>50</sup> Using the properties of this dimer as a PDT photosensitized and a fluorescent ratiometric molecular rotor, monitor the initiation of cell death via irradiation and changes in intracellular viscosity of light-perturbed single cells.

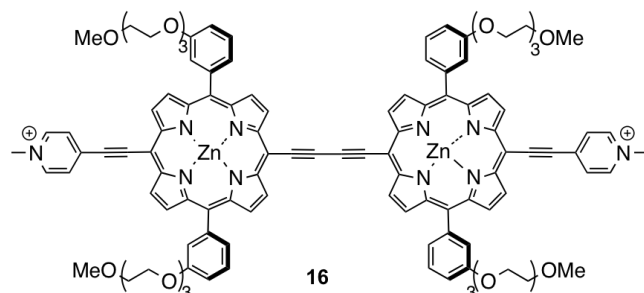


Fig. 9. Chemical structure of porphyrin dimer 16

An alternative design of a single TICT fluorophore with dual emission profile is based on tautomerism. Thus, the isoquinoline derivative MDP-BIQ (**17**, Fig. 10) shows dual fluorescence with band positions and intensities that are solvent dependent.<sup>51</sup> The dual fluorescence arises from the two valence tautomers of this compound, one aromatic and one conjugated but not aromatic, each of which exhibit different fluorescent characteristics. The relatively high fluorescence quantum yield of the aromatic tautomer (0.123 versus 0.002 for the non-aromatic tautomer) makes this molecule interesting for use in sensors and other optoelectronic applications. Similarly, 3-hydroxy chromone dyes (such as **18**, Fig. 10) exhibit two well-separated emission bands that allow a self-calibrating behavior for sensing of polarity, hydrogen bonding ability and local electrostatic fields.<sup>52</sup> This property has been explored for measurements of viscosity and polarity in lipid bilayers and membranes.<sup>53</sup>

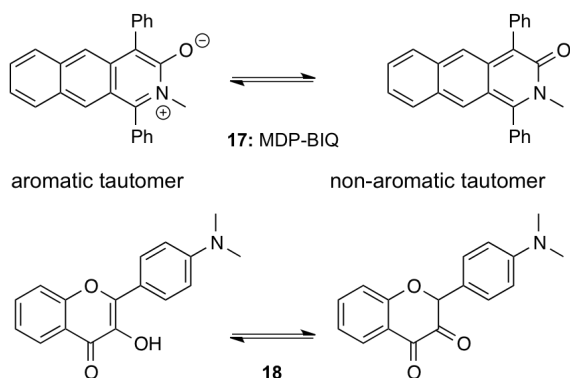


Fig. 10. Representative structures of TICT fluorophores that exhibit dual fluorescence emission due to tautomerism.

3-hydroxy chromone dyes are characterized by a reversible excited state intramolecular proton transfer (ESIPT) ability that, in lipid bilayers, produces two different ground state forms: (a) the H-bonded form with water (hydrated) and (b) the non-H-bonded form (non-hydrated) that exhibit different fluorescence excitation and emission characteristics (Fig. 11).<sup>53</sup> The non-hydrated form exhibits a dual emission as in aprotic solvents, while the H-bonded form exhibits a single emission similar to the spectra obtained in protic solvents. Deconvolution of their spectra in three bands provides

information on the contribution of the hydrated form defined as the ratio of HN\* to the sum of N\*+T\* bands. Moreover, the N\*/T\* ratio can be used as a polarity indicator. Similar solvatochromic effects based on intramolecular proton transfer have been reported for benzofluorenones.<sup>54</sup>

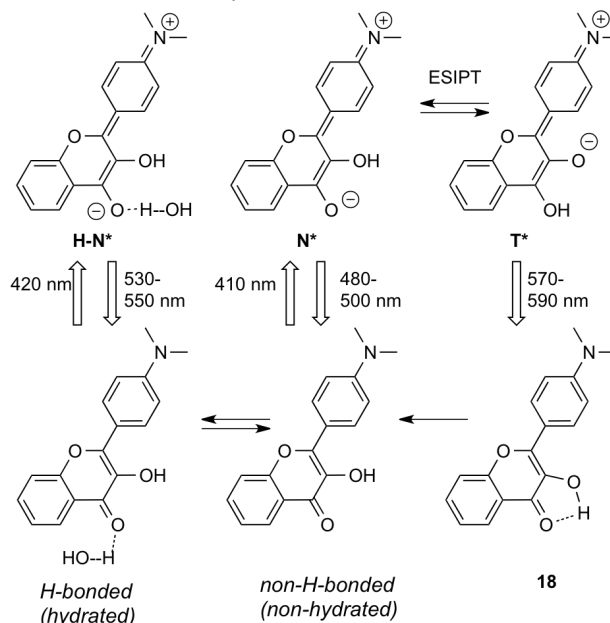
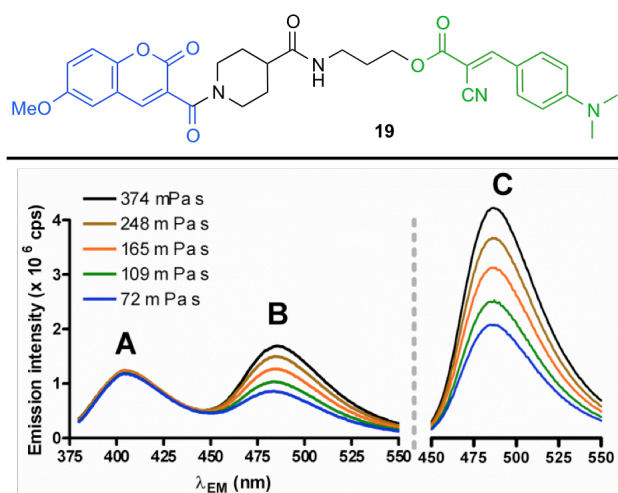


Fig. 11. Ground (bottom) and excited (top) states of 3-hydroxy chromone derivatives in lipid bilayers. Upward arrows indicate excitation and downward arrows indicate emission.

## 5. TICT fluorophores linked to an internal reference dye

An attractive concept is to combine an environment-sensitive dye with a reference fluorophore that is not environment-sensitive or at least shows different sensitivity. A good example for this concept was provided by Luby-Phelps *et al.*<sup>55</sup> who measured intracellular viscosity by examining the emission ratio of two dyes with slightly different chemical structure such as Cy3 and Cy5. In this case, Cy3 acts as viscosity-sensitive fluorophore while the more rigid Cy5 acts as the viscosity-insensitive reference. This study shows that the emission ratio of Cy3 to Cy5 increases almost 3-fold with a 30-fold viscosity increase although the relationship is nonlinear. Inside the cell cytoplasm, the Cy3-Cy5 system indicates viscosities only slightly higher than pure PBS. Albeit innovative, this approach is limited by the assumption that the two dyes exist in equal concentration in a given environment. In turn, this restricts its application to measuring viscosity changes in homogeneous environments.

The above limitation can be circumvented by covalently linking an environment-sensitive fluorophore with a reference fluorophore. Compound **19** illustrates this concept where a ratiometric viscosity dye is produced by conjugating a viscosity-insensitive coumarin dye (internal reference) with a fluorescent molecular rotor (viscosity sensitive) (Fig. 12).<sup>56</sup> This design is further discussed in the following section.



**Fig. 12. Top panel:** Chemical structure of a representative ratiometric viscosity dye where a coumarin fluorophore (blue fragment) is covalently bound to a TICT fluorophore (green fragment). **Bottom panel:** Emission spectra of dye **19** in mixtures of ethylene glycol and glycerol. Peak A represents coumarin emission and peak B rotor emission through RET excitation from coumarin. Peaks A and B were acquired at the same excitation wavelength ( $\lambda_{\text{ex}} = 360$  nm). Peak C is the emission from direct excitation of the TICT fluorophore at  $\lambda_{\text{ex}} = 444$  nm. Only peaks B and C are viscosity-dependent.

The above concept was taken further toward the development of a mitochondria-specific bipartite viscosity sensor (Fig. 13).<sup>57</sup> Compound **20** is composed of three parts: (a) a phosphonium cation for localization in mitochondria, (b) a coumarin dye that acts as a viscosity insensitive reference dye and (c) a phenyl-substituted boron-dipyrrromethene (BODIPY) unit that acts as the viscosity-sensitive unit. Use of a phenyl ring as a linker between the BODIPY and the coumarin offers two advantages: (a) it maintains the distance and relative orientation of the coumarin and BODIPY units; and (b) it allows an efficient through-bond energy transfer.<sup>58</sup> The sensor showed a direct linear relationship between the fluorescence intensity ratio of BODIPY to coumarin or the fluorescence lifetime ratio and the media viscosity. Specifically, it showed two emission peaks at 427 and 516 nm that were both viscosity-sensitive, the red-shifted emission being considerably more sensitive to viscosity changes. Plotting the intensity ratio of the two bands versus the solvent viscosity revealed a direct linear relationship ( $R^2 = 0.995$ ) indicating that compound **20** meets the necessary criteria for a ratiometric viscosity sensor. Similarly, a linear relationship was found between the lifetime of **20** at 516 and the solvent viscosity ( $R^2 = 0.997$ ). Using this compound, the authors determined the average mitochondrial viscosity of living cells as ca 62 cP. Treatment of these mitochondria with an ionophore, e.g. monensin, increased mitochondria viscosity to ca 110 cP.

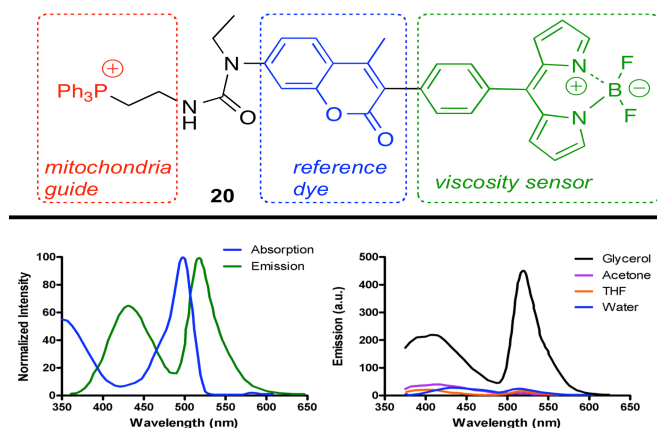


**Fig. 13. Top panel:** Chemical structure of a mitochondria-specific ratiometric fluorescent viscosity sensor (**20**). This compound is composed by covalently linking a mitochondria guide (red fragment) with a reference dye (blue fragment) and a viscosity sensor (green fragment). **Bottom panel:** Normalized absorption and fluorescence spectra (A) of **20** in methanol and (B) fluorescence response in different solvents when excited at 330 nm.<sup>57</sup>

The near infrared BODIPY probe **21** emits at 720 nm and shows strong quenching in the presence of copper (+2) due to photon-induced electron transfer to the copper ion (Fig. 14).<sup>59</sup> Although other mono or divalent metals have little effect on the absorption and emission spectra of **21**, a new fluorescence band was detected at 580 nm in the presence of aluminium (+3). It was proposed that this blue-shifted band is caused by selective binding of the aluminium ion to the piperidinobenzyl group of the sensor.

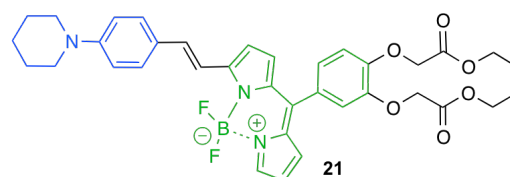


**Fig. 14. Representative example of a selective  $\text{Cu}^{2+}$  and  $\text{Al}^{3+}$  ion sensor.** Presence of  $\text{Cu}^{2+}$  quenches the fluorescence due to photon-induced electron transfer to the copper ion that preferentially binds to the BODIPY group (green motif). The  $\text{Al}^{3+}$  ion is hypothesized to be attracted to the piperidinobenzyl group (blue motif), where it facilitates an additional ICT deexcitation pathway with blue-shifted emission.

## 6. Rational design of ratiometric mechanosensitive TICT fluorophores

The underlying idea for the dual-emission dyes covered in this article is to provide an artificial reference by covalently linking a fluorescent molecular rotor to a viscosity-insensitive reference fluorophore as shown in Fig. 15. Emission from the reference is subject to the same factors as emission from the molecular rotor,  $I_{\text{ref}} = I_{\text{ex}} \cdot c \cdot g \cdot \Phi_{\text{ref}}$  where  $\Phi_{\text{ref}}$  is the quantum yield of the reference fluorophore and usually  $\Phi_{\text{ref}} \approx 1$ . While this property holds for the dual-emission dyes in the previous section, our rationale is to allow more design flexibility in the design of a ratiometric sensing system.

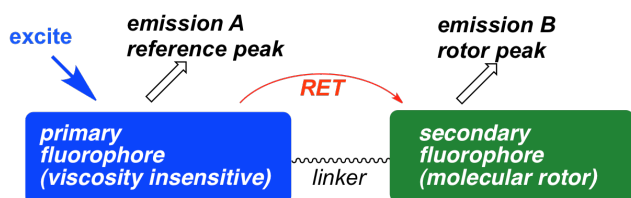


Fig. 15. General design of ratiometric TICT mechanosensitive dyes based on the resonance energy transfer concept.

To keep the emission spectra as simple as possible, the fluorescent molecular rotor is preferentially of the kind that shows only emission from the planar conformation and exhibits radiationless deexcitation in the twisted conformation. This type of dye adheres to Equation 3 with emission from its single band. Moreover, LE emission is known to be less sensitive to solvent polarity than TICT emission, because the excited-state dipole moment is lower in the planar conformation. The resulting engineered dual-emission dyes are therefore relatively robust against changes in the environment polarity.<sup>38a, 41, 60</sup>

**Theory:** When we consider Equation 3, viscosity measurements rely on the accurate determination of the quantum yield. As one option, fluorescence lifetime measurements yield the solvent viscosity by combining Equations 3 and 4, and solving for the viscosity  $\eta$ :

$$\eta = \sigma \cdot \left( \frac{\tau}{\tau_N \Phi_0} \right)^{1/x} = C \cdot \tau^{1/x} \quad (5)$$

where the different dye-dependent constants  $\sigma$ ,  $\tau_N$ , and  $\Phi_0$  can be interpreted as calibration constants (much like the geometry and sensor properties of a mechanical rheometer) and combined into a single calibration constant  $C$ . In steady-state spectroscopy, no such straightforward relationship exists. However, a ratiometric measurement with reference emission yields the molecular rotor quantum yield when Equation 2 is solved for  $\Phi_F$ . Similar to lifetime measurements, the quantum yield obtained in this fashion can be used in Equation 3 to obtain solvent viscosity, but this measurement can be provided using lower-cost steady-state instruments. Moreover, the ratio  $I_{em}/I_{ref}$  can be related to the solvent viscosity by nonlinear regression, and the relationship in Equation 6 can generally be found:

$$\frac{I_{em}}{I_{ref}} = C \cdot \eta^x \quad (6)$$

Similar to Equation 5, the constants  $C$  and  $x$  can be interpreted as calibration constants and obtained from the model solvents. When the environment whose viscosity is probed has similar properties as the calibration solvent, the constants  $C$  and  $x$  remain valid, and viscosity can be obtained by solving Equation 6 for  $\eta$ .

One key assumption that has been made is negligible absorption of emission light by the solvent. If the absorption at the rotor and reference emission wavelengths is

approximately the same, Equation 6 is still valid. However, if the solvent shows clear coloration, measurements should be taken to determine absorbance or molar extinction coefficients at the rotor and reference emission wavelengths, respectively. A correction is possible, but due to the nonlinear nature of light absorption (Lambert-Beer's law), the geometry now plays a role. Specifically, if the absorption of the solvent at the rotor wavelength is  $A_F$  and the absorption at the reference wavelength is  $A_{ref}$ , Equation 6, solved for  $\eta$  and given in logarithmic form, expands to

$$\ln \eta = \frac{d}{x} (A_F - A_{ref}) + \frac{1}{x} \ln \left( \frac{1}{C} \cdot \frac{I_{em}}{I_{ref}} \right) \quad (7)$$

where  $d$  is the distance that the emission light travels through the absorbing material. Because of these additional and usually unknown variables, equation 7 is no longer useful in practice. However, if the assumption of either  $A_F \approx A_{ref}$  or  $d \rightarrow 0$  can be made, we return to Equation 6.

**Resonance energy transfer:** One of the most fundamental properties to consider when the rotor and reference fluorophore are brought in close proximity by covalent linking is resonance energy transfer (RET). One design strategy would aim to minimize energy transfer, but a second avenue is to make energy transfer integral part of the fluorophore design.

**Minimizing energy transfer:** To minimize energy transfer, either the dipole-dipole distance  $r$  needs to be maximized, or the spectral overlap  $J$  needs to be minimized. Maximizing the distance  $r$  requires the use of a long and rigid linker structure, i.e., an organic chain that does not fold back onto itself. A longer linker structure will lead to a bulkier molecule, and it decreases solubility. Minimizing the spectral overlap requires a choice of rotor and reference dyes with strongly diverging spectral properties. For example, a typical fluorescent molecular rotor has a peak excitation in the violet or blue range and blue-green emission. Far-UV excitation is often impractical, and the choice would be to minimize the spectral overlap by using a red-excited dye such as Texas Red or Rhodamine 800.

Alternatively, a reference dye can be used that has a very large Stokes shift, but an excitation peak similar to that of the molecular rotor. For example, Lucifer Yellow (excitation near 420 nm, emission peak at 540 nm) can be used with CCVJ derivatives (excitation near 405 nm, emission peak at 470 nm). The disadvantage of this method is the overlap of the emission spectra; notably reference fluorophores with very high quantum yield contribute significant emission to the molecular rotor peak. Similarly, a fluorescent molecular rotor with a very large Stokes shift (e.g. 27) can be used.

**Making energy transfer part of the fluorophore design:** We found that energy transfer can be desirable for two reasons. First, it allows measurement of the two emission spectra with one single excitation source and thus with a single measurement (Fig. 15). Second, fluorescent molecular rotors are usually characterized by a very low quantum yield, unlike most environment-insensitive reference dyes whose quantum

yield is near unity. With RET, relatively short linker structures are acceptable. In fact, the dipole-dipole distance  $r$  may be smaller than the Förster distance  $R_0$  with the consequence of a high energy transfer  $E \approx 1$ . For example,  $E = 0.999$  indicates that 99.9% of the excited energy of the reference fluorophore is transferred to the fluorescent molecular rotor and only 0.1% of the energy is measurable as reference emission. When we consider the typical quantum yield of a molecular rotor in low-viscosity solvents, the two emission intensities are balanced. This is a desirable property.

In this context, the reference dye is restricted to a role as RET donor. If this is not the case (i.e., the donor is the molecular rotor), the Förster distance, which depends on the donor quantum yield also depends on the viscosity.<sup>13</sup> Therefore, the reference would become viscosity-dependent as well, which violates our fundamental assumption.

**Modifications of the chemical structure:** The spectral properties of both the reference moiety and the molecular rotor can be modified by chemical substitution of their functional groups. Often, the reference dye is selected from commercially available fluorescent labels with reactive groups (e.g., NHS ester). The linker unit between molecular rotor and the reference fluorophore can be adapted to specific functions as well. The basic C3 linker structure in **22** can be substituted for longer chains (e.g. 5, 6, or 8 carbon atoms) that permit lower energy transfer and thus, higher emission from the reference dye.<sup>61</sup> Since long linkers may lead to folding of the dye system, rigidifying the linker with unsaturated chains or rings (e.g. **19**) may be beneficial. In fact, the balance of reference and rotor peak between **19** and **22** is similar.<sup>56b</sup> On the other hand, the use of a triethyleneglycol motif (e.g. **23**) increases water-solubility, but at the same time decreases energy transfer. Compared with **19** and **22**, dye **23** shows strongly enhanced reference emission and reduced viscosity sensitivity (Fig. 16).<sup>62</sup>

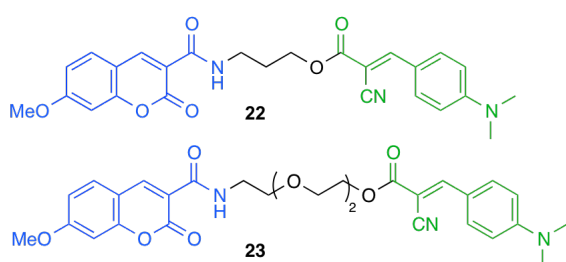


**Fig. 16. Ratiometric TICT mechanosensitive dyes with various linkers.** The saturated hydrocarbon chain of **22** creates a hydrophobic dye, whereas the triethyleneglycol motif of **23** facilitates water solubility.

Structural modifications of the molecular rotor unit have been reported that lead to higher quantum yield or larger Stokes shift.<sup>63</sup> The basic structure for a single-emission molecular rotor is dicyanovinyl *N,N*-dimethylaniline (**25**, Fig. 17). Replacing the aniline core of **25** with a tricyclic julolidine motif yields DCVJ (**10**) with a slightly higher quantum yield. It is possible to replace one of the nitrile groups of **25** with a

carboxyl group (e.g. **26**) and use esterification to attach the other components of the ratiometric dye (i.e., linker and reference fluorophore). The remaining nitrile group becomes the dominant ICT electron acceptor, and the primary bond of intramolecular rotation remains the vinyl-benzene single bond. More pronounced changes of the photophysical behavior are observed when the  $\pi$ -conjugation system is modified. For instance, replacing the benzene ring of **26** with a thiophene ring (e.g. **28**) leads to a strong increase of the quantum yield with almost no change to viscosity sensitivity and a minor bathochromic shift of excitation (30 nm) and emission (15 nm).<sup>63-64</sup> Increasing the spatial separation of the ICT electron donor and acceptor groups causes a small bathochromic shift of the peak excitation wavelength, but a major bathochromic shift of the emission wavelength. For example, replacement of benzene by naphthalene in the basic molecular rotor structure yields viscosity-sensitive dye **27** with peak emission at 598 nm.<sup>63</sup> The quantum yield of **27** is about ten-fold higher than that of DCVJ, although its sensitivity (i.e., the exponent  $x$ ) is reduced. Such dyes can be combined with a green-emitting reference into a single-excitation dye system that does not rely on resonance energy transfer.

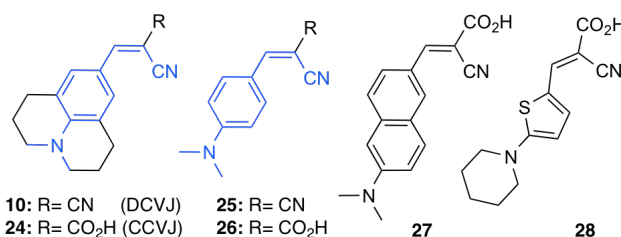


**Fig. 17. Structural modifications of the fluorescent molecular rotor.** The basic structure of a single emission fluorescent rotor is shown in blue. Substitution of one nitrile group for a carboxyl group improves water solubility and creates an attachment point for functional groups (**24**, **26**). Increasing the spatial distance between ICT electron donor and acceptor (**27**) causes a very strong bathochromic shift of the emission spectrum. Substitution of the benzene for a thiophene (**28**) increases the overall quantum yield without reducing sensitivity.

In a limited study, no significant effect was found when the dimethylamino group that serves as ICT donor is replaced by longer-chained groups, i.e., diethylamino or dibutylamino.<sup>63</sup> It appears possible that the donor group can be modified to provide reactive groups as well, at which functional groups can be linked. For example, a membrane-compatible ratiometric dye can be envisioned that features aliphatic chains similar to those of phospholipid molecules. On the other hand, a more hydrophilic molecular rotor can be created when both nitrile groups are replaced by carboxy groups, leading to a dicarbocvinylianiline fluorophore.<sup>65</sup> In this case, a hydrophilic linker would be attached to the amine to complete the ratiometric dye. One additional consideration is the recently observed formation of photoisomers.<sup>65-66</sup> As soon as the ICT electron acceptor is asymmetric (for example, in CCVJ), light exposure rapidly leads to the formation of an isomer of lower quantum yield. In steady-state spectroscopy, photoisomerization occurs rapidly, resulting in only one dominant specimen. However, for time-resolved

measurements of quantum yield with slow alternating levels of ambient or excitation light (with light fluctuations in the order of seconds to hours), the equilibrium of isomers will change, and the measurement will be influenced by the light-dark ratio.

## 7. Conclusions

Fluorescent probes have evolved into molecular-sized sensors that allow highly accurate quantitative measurements. Three key metrics play a role: Emission wavelength (usually influenced by the environment's polarity),<sup>67</sup> fluorescent quantum yield (influenced by quenching, protonation or other environmental factors), and fluorescent lifetime. The latter two are linearly related, and time-resolved spectroscopy can serve to accurately measure the quantum yield. Conversely, steady-state spectroscopy depends on several factors other than quantum yield. In the case of molecular rotors, whose quantum yield depends on the environment's microviscosity, measurement precision is limited to relative measurements. One approach to eliminate those external factors, the use of a second emission band, has gained recent popularity. Fluorescent molecular rotors can be designed to have two emission bands, whose ratio cancels out the external factors. Alternatively, a dye system can be constructed that consists of a molecular rotor and a non-sensitive reference unit. Such dye combinations have been shown to provide viscosity in actual physical units of mPa·s.<sup>68</sup> More recently, similar dye systems have been introduced that are based on BODIPY sensing units. These dye systems allow a high degree of flexibility in their chemical structure, and they can be targeted to specific environments. As such, they promise new applications as quantitative reporters in cell membranes,<sup>53, 69</sup> for bulk fluids,<sup>70</sup> for polymerization dynamics<sup>39c</sup> and whole body imaging.

## 8. Acknowledgements

Financial support from the National Institutes of Health (1R21 RR025358, MAH) and the Cancer Research Coordinating Committee (CRC-15-380737, EAT) is gratefully acknowledged. We thank the National Science Foundation for instrumentation grants CHE9709183 and CHE0741968.

## Notes and references

1. B. Valeur and M. N. Berberan-Santos, *J. Chem. Educ.*, 2011, 88, 731-738.
2. G. G. Stokes, *Phil. Trans. R. Soc. Lond.*, 1852, 142, 463-562.
3. V. Pierre, *Sitzber. Boehm. Ges. Wiss. Prag.*, 1862, 2, 66 -82.
4. F. Goppelsroeder, *J. Prakt. Chem.*, 1868, 104, 10-27.
5. M. Zimmer, *Chem. Soc. Rev.*, 2009, 38, 2823-2832.
6. L. Mockl, D. C. Lamb and C. Brauchle, *Angew. Chem. Int. Ed.*, 2014, 53, 13972-13977.
7. a) D. M. Chudakov, M. V. Matz, S. Lukyanov and K. A. Lukyanov, *Physiol. Rev.*, 2010, 90, 1103-1163; b) M. Schaferling, *Angew. Chem. Int. Ed.*, 2012, 51, 3532-3554; c) S. N. Uno, M. Kamiya, T. Yoshihara, K. Sugawara, K. Okabe, M. C. Tarhan, H. Fujita, T. Funatsu, Y. Okada, S. Tobita and Y. Urano, *Nat. Chem.*, 2014, 6, 681-689; d) D. S. Liu, L. G. Nivon, F. Richter, P. J. Goldman, T. J. Deerinck, J. Z. Yao, D. Richardson, W. S. Phipps, A. Z. Ye, M. H. Ellisman, C. L. Drennan, D. Baker and A. Y. Ting, *Proc. Natl. Acad. Sci. USA*, 2014, 111, E4551-E4559; e) E. Kim, Y. Lee, S. Lee and S. B. Park, *Acc. Chem. Res.*, 2015, 48, 538-547.
8. a) R. S. Balaban and V. A. Hampshire, *ILAR Journal / National Research Council, Institute of Laboratory Animal Resources*, 2001, 42, 248-262; b) M. de Jong, J. Essers and W. M. van Weerden, *Nat. Rev. Cancer*, 2014, 14, 481-493; c) M. M. Khalil, J. L. Tremoleda, T. B. Bayomy and W. Gsell, *Int. Journal Mol. Imaging*, 2011, 2011, 796025; d) W. Koba, L. A. Jelicks and E. J. Fine, *Am. J. Pathol.*, 2013, 182, 319-324; e) F. Leblond, S. C. Davis, P. A. Valdes and B. W. Pogue, *J. Photochem. Photobiol. B*, 2010, 98, 77-94; f) Y. Engelborghs and A. J. W. G. Visser, *Meth. Mol. Biol.*, 2014, 1076, V-Xii.
9. R. Weissleder and M. J. Pittet, *Nature*, 2008, 452, 580-589.
10. A. P. Demchenko, in *Springer Series on Fluorescence, Methods and Applications 8*, Springer, Berlin; Heidelberg, 2010.
11. A. W. Czarnik, *Acc. Chem. Res.*, 1994, 27, 302-308.
12. a) M. A. Haidekker, M. Nipper, A. Mustafic, D. Lichlyter, M. Dakanali and E. A. Theodorakis, *Springer Ser. Fluores.*, 2010, 8, 267-308; b) M. A. Haidekker and E. A. Theodorakis, *Org. Biomol. Chem.*, 2007, 5, 1669-1678.
13. J. R. Lakowicz, *Principles of fluorescence spectroscopy*, Springer, New York, 3rd edn., 2006.
14. a) G. Weber and F. J. Farris, *Biochemistry-US*, 1979, 18, 3075-3078; b) E. K. Krasnowska, E. Gratton and T. Parasassi, *Biophys. J.*, 1998, 74, 1984-1993.
15. a) J. J. Ory and L. J. Banaszak, *Biophys. J.*, 1999, 77, 1107-1116; b) A. V. Pastukhov and I. J. Ropson, *Proteins*, 2003, 53, 607-615.
16. B. C. Lobo and C. J. Abelt, *J. Phys. Chem. A*, 2003, 107, 10938-10943.
17. T. Parasassi, G. De Stasio, A. Dubaldo and E. Gratton, *Biophys. J.*, 1990, 57, 1179-1186.
18. P. Valat, V. Wintgens, J. Kossanyi, L. Biczok, A. Demeter and T. Berces, *J. Am. Chem. Soc.*, 1992, 114, 946-953.
19. a) P. Nandhikonda and M. D. Heagy, *Org. Lett.*, 2010, 12, 4796-4799; b) P. Nandhikonda and M. D. Heagy, *Chem. Commun.*, 2010, 46, 8002-8004; c) P. Nandhikonda and M. D. Heagy, *J. Am. Chem. Soc.*, 2011, 133, 14972-14974.
20. a) S. Banerjee, E. B. Veale, C. M. Phelan, S. A. Murphy, G. M. Tocci, L. J. Gillespie, D. O. Frimannsson, J. M.

- Kelly and T. Gunnlaugsson, *Chem. Soc. Rev.*, 2013, 42, 1601-1618; b) M. P. Begaye, P. Nandhikonda, Z. Cao and M. D. Heagy, *Rev. Fluoresc.*, 2010, 5, 461-477; c) Z. Cao, P. Nandhikonda, A. Penuela, S. Nance and A. D. Heagy, *Int. J. Photoenergy*, 2010, DOI: Artn 26464310.1155/2010/264643; d) R. M. Duke, E. B. Veale, F. M. Pfeffer, P. E. Kruger and T. Gunnlaugsson, *Chem. Soc. Rev.*, 2010, 39, 3936-3953; e) I. Grabchev, S. Dumas and J. M. Chovelon, *Dyes Pigments*, 2009, 82, 336-340.
21. a) P. Nandhikonda, M. P. Begaye, Z. Cao and M. D. Heagy, *Chem. Commun.*, 2009, 4941-4943; b) P. Nandhikonda, M. P. Begaye, Z. Cao and M. D. Heagy, *Org. Biomol. Chem.*, 2010, 8, 3195-3201; c) P. Nandhikonda, Z. Cao and M. D. Heagy, *Rev. Fluoresc.*, 2011, 6, 303-319; d) P. Nandhikonda, S. Paudel and M. D. Heagy, *Tetrahedron*, 2009, 65, 2173-2177; e) S. Paudel, P. Nandhikonda and M. D. Heagy, *J. Fluoresc.*, 2009, 19, 681-691.
22. X. Zhang and Y. B. Jiang, *Photoch. Photobio. Sci.*, 2011, 10, 1791-1796.
23. G. Eber, F. Gruneis, Schneide.S and F. Dorr, *Chem. Phys. Lett.*, 1974, 29, 397-404.
24. R. Y. Tsien and M. Poenie, *Trends Biochem. Sci.*, 1986, 11, 450-455.
25. a) S. Deo and H. A. Godwin, *J. Am. Chem. Soc.*, 2000, 122, 174-175; b) C. T. Chen and W. P. Huang, *J. Am. Chem. Soc.*, 2002, 124, 6246-6247.
26. a) G. K. Walkup, S. C. Burdette, S. J. Lippard and R. Y. Tsien, *J. Am. Chem. Soc.*, 2000, 122, 5644-5645; b) Z. C. Xu, J. Yoon and D. R. Spring, *Chem. Soc. Rev.*, 2010, 39, 1996-2006.
27. Z. C. Xu, Y. Xiao, X. H. Qian, J. N. Cui and D. W. Cui, *Org. Lett.*, 2005, 7, 889-892.
28. R. W. Sinkeldam, N. J. Greco and Y. Tor, *Chem. Rev.*, 2010, 110, 2579-2619.
29. Y. Zhou and J. Yoon, *Chem. Soc. Rev.*, 2012, 41, 52-67.
30. K. McCluskey, E. Shaw, D. Lafontaine and J. C. Penedo, in *Fluorescence Spectroscopy and Microscopy*, eds. Y. Engelborghs and A. J. W. G. Visser, Humana Press, 2014, vol. 1076, ch. 35, pp. 759-791.
31. H. S. Cao and M. D. Heagy, *J. Fluoresc.*, 2004, 14, 569-584.
32. F. Galindo, J. Becerril, M. I. Burguete, S. V. Luis and L. Vigarra, *Tetrahedron Lett.*, 2004, 45, 1659-1662.
33. D. W. Shen, M. F. Bai, R. Tang, B. G. Xu, X. M. Ju, R. G. Pestell and S. Achilefu, *Sci. Rep.-UK*, 2013, 3.
34. Z. R. Grabowski, K. Rotkiewicz and W. Rettig, *Chem. Rev.*, 2003, 103, 3899-4031.
35. E. Lippert, W. Luder and H. Boos, *Advances in Molecular Spectroscopy*, 1962, 443-457.
36. K. Rotkiewicz, K. H. Grellmann and Z. R. Grabowski, *ChemPhysLett*, 1973, 17, 315-318.
37. T. Förster and G. Hoffmann, *Zeitschrift Phys. Chem*, 1971, 75, 63-76.
38. a) C. E. Kung and J. K. Reed, *Biochemistry-UU*, 1986, 25, 6114-6121; b) M. L. Viriot, M. C. Carre, C. Geoffroy-Chapotot, A. Brembilla, S. Muller and J. F. Stoltz, *Clin. Hemorheol. Micro.*, 1998, 19, 151-160; c) S. Lukac, *J. Am. Chem. Soc.*, 1984, 106, 4386-4392; d) M. E. Nipper, S. Majd, M. Mayer, J. C. M. Lee, E. A. Theodorakis and M. A. Haidekker, *BBA-Biomembranes*, 2008, 1778, 1148-1153.
39. a) R. O. Loutfy and B. A. Arnold, *J. Phys. Chem-US*, 1982, 86, 4205-4211; b) R. O. Loutfy, *Macromolecules*, 1983, 16, 678-680; c) D. H. Zhu, M. A. Haidekker, J. S. Lee, Y. Y. Won and J. C. M. Lee, *Macromolecules*, 2007, 40, 7730-7732.
40. a) C. E. Kung and J. K. Reed, *Biochemistry-US*, 1989, 28, 6678-6686; b) A. Hawe, V. Filipe and W. Jiskoot, *Pharm. Res.-Dord*, 2010, 27, 314-326.
41. B. D. Allen, A. C. Benniston, A. Harriman, S. A. Rostron and C. F. Yu, *Phys. Chem. Chem. Phys.*, 2005, 7, 3035-3040.
42. R. O. Loutfy and K. Y. Law, *J. Phys. Chem.-US*, 1980, 84, 2803-2808.
43. M. K. Kuimova, G. Yahioglu, J. A. Levitt and K. Suhling, *J. Am. Chem. Soc.*, 2008, 130, 6672-+.
44. B. Albinsson, *J. Am. Chem. Soc.*, 1997, 119, 6369-6375.
45. A. D. Welland, F. W. Schneider and A. B. J. Parusel, *Chem. Phys.*, 1999, 240, 403-411.
46. V. Thiagarajan, C. Selvaraju, E. J. P. Malar and P. Ramamurthy, *ChemPhysChem*, 2004, 5, 1200-1209.
47. X. J. Peng, Z. G. Yang, J. Y. Wang, J. L. Fan, Y. X. He, F. L. Song, B. S. Wang, S. G. Sun, J. L. Qu, J. Qi and M. Yang, *J. Am. Chem. Soc.*, 2011, 133, 6626-6635.
48. A. Ito, S. Ishizaka and N. Kitamura, *Phys. Chem. Chem. Phys.*, 2010, 12, 6641-6649.
49. a) J. W. Zhang, J. T. Luo, X. X. Zhu, M. J. N. Junk and D. Hinderberger, *Langmuir*, 2010, 26, 2958-2962; b) A. P. Davis and J. B. Joos, *Coordin. Chem. Rev.*, 2003, 240, 143-156; c) L. J. Lawless, A. G. Blackburn, A. J. Ayling, M. N. Perez-Payan and A. P. Davis, *J. Chem. Soc. Perkin Trans. 1*, 2001, 1329-1341.
50. M. K. Kuimova, S. W. Botchway, A. W. Parker, M. Balaz, H. A. Collins, H. L. Anderson, K. Suhling and P. R. Ogilby, *Nat. Chem.*, 2009, 1, 69-73.
51. I. M. Craig, H. M. Duong, F. Wudl and B. J. Schwartz, *Chem. Phys. Lett.*, 2009, 477, 319-324.
52. A. P. Demchenko, *Febs Lett.*, 2006, 580, 2951-2957.
53. A. P. Demchenko, Y. Mely, G. Duportail and A. S. Klymchenko, *Biophys. J.*, 2009, 96, 3461-3470.
54. W. J. Yang and X. B. Chen, *Phys. Chem. Chem. Phys.*, 2014, 16, 4242-4250.
55. K. Lubyphelps, S. Mujumdar, R. B. Mujumdar, L. A. Ernst, W. Galbraith and A. S. Waggoner, *Biophys. J.*, 1993, 65, 236-242.
56. a) D. Fischer, E. A. Theodorakis and M. A. Haidekker, *Nat. Protoc.*, 2007, 2, 227-236; b) M. A. Haidekker, T. P. Brady, D. Lichlyter and E. A. Theodorakis, *J. Am. Chem. Soc.*, 2006, 128, 398-399.

57. Z. Yang, Y. He, J. H. Lee, N. Park, M. Suh, W. S. Chae, J. F. Cao, X. J. Peng, H. Jung, C. Kang and J. S. Kim, *J. Am. Chem. Soc.*, 2013, 135, 9181-9185.
58. Y. J. Gong, X. B. Zhang, C. C. Zhang, A. L. Luo, T. Fu, W. H. Tan, G. L. Shen and R. Q. Yu, *Anal. Chem.*, 2012, 84, 10777-10784.
59. X. J. Xie and Y. Qin, *Sensor Actuat. B-Chem.*, 2011, 156, 213-217.
60. a) M. A. Haidekker, T. P. Brady, S. H. Chalian, W. Akers, D. Lichlyter and E. A. Theodorakis, *Bioorg. Chem.*, 2004, 32, 274-289; b) M. A. Haidekker, T. P. Brady, D. Lichlyter and E. A. Theodorakis, *Bioorg. Chem.*, 2005, 33, 415-425.
61. H. J. Yoon, M. Dakanali, D. Lichlyter, W. M. Chang, K. A. Nguyen, M. E. Nipper, M. A. Haidekker and E. A. Theodorakis, *Org. Biomol. Chem.*, 2011, 9, 3530-3540.
62. M. Dakanali, T. H. Do, A. Horn, A. Chongchivivat, T. Jarusreni, D. Lichlyter, G. Guizzunti, M. A. Haidekker and E. A. Theodorakis, *Bioorg. Med. Chem.*, 2012, 20, 4443-4450.
63. J. Sutharsan, D. Lichlyter, N. E. Wright, M. Dakanali, M. A. Haidekker and E. A. Theodorakis, *Tetrahedron*, 2010, 66, 2582-2588.
64. L. S. Kocsis, K. M. Elbel, B. A. Hardigree, K. M. Brummond, M. A. Haidekker and E. A. Theodorakis, *Org. Biomol. Chem.*, 2015, 13, 2965-2973.
65. A. Mustafic, K. M. Elbel, E. A. Theodorakis and M. Haidekker, *J. Fluoresc.*, 2015, 25, 729-738.
66. C. Rumble, K. Rich, G. He and M. Maroncelli, *J. Phys. Chem. A*, 2012, 116, 10786-10792.
67. a) E. Lippert, *Z Elektrochem*, 1957, 61, 962-975; b) N. Mataga, Y. Kaifu and M. Koizumi, *Bull. Chem. Soc. Jpn.*, 1956, 29, 465-470.
68. M. E. Nipper, M. Dakanali, E. Theodorakis and M. A. Haidekker, *Biochimie*, 2011, 93, 988-994.
69. A. S. Klymchenko and R. Kreder, *Chem. Biol.*, 2014, 21, 97-113.
70. W. J. Akers and M. A. Haidekker, *J. Biomech. Eng. -T ASME*, 2005, 127, 450-454.

